

Studies of the interaction of CS@ZnS:Mn with bovine serum albumin under illumination



Li Liu^{a,*}, Ling Xiao^b

^a Institute of Agricultural Quality Standards and Testing Technology Research, Hubei Academy of Agricultural Science, Wuhan 430064 PR China

^b School of Resource and Environmental Science, Hubei Biomass-Resource Chemistry and Environmental Biotechnology Key Laboratory, Wuhan University, Wuhan 430072 PR China

ARTICLE INFO

Article history:

Received 7 December 2014

Received in revised form 23 April 2015

Accepted 29 April 2015

Available online 6 May 2015

Keywords:

Doped semiconductor nanocrystals

Chitosan

Bovine serum albumin

Interaction

UV illumination

ABSTRACT

In this study, chitosan coated Mn-doped ZnS quantum dots (CS@ZnS:Mn D-dots) were obtained in aqueous media under ambient pressure. The interaction and illumination damages of CS@ZnS:Mn D-dots with bovine serum albumin (BSA) were studied by means of ultraviolet–visible (UV–vis) and fluorescence (FL) spectra. It was found that the FL of BSA was quenched by CS@ZnS:Mn D-dots. The dominating quenching mechanism of CS@ZnS:Mn D-dots with BSA belongs to dynamic quenching. Hydrophobic interaction plays a major role in the CS@ZnS:Mn–BSA interaction; binding processes are spontaneous. Influencing factors such as illumination time and CS@ZnS:Mn D-dots concentrations were considered. The FL quenching effect of BSA by CS@ZnS:Mn D-dots is enhanced with the increase of illumination time and CS@ZnS:Mn D-dots concentration. The FL enhancement of CS@ZnS:Mn D-dots by BSA under UV illumination was also observed. It was proved that, the interaction of CS@ZnS:Mn D-dots with BSA under UV illumination is mainly a result of a photo-induced free radical procedure. CS@ZnS:Mn D-dots may be used as photosensitizers in photodynamic therapy.

© 2015 Elsevier B.V. All rights reserved.

1. Introduction

Semiconductor nanocrystals, also named quantum dots (Q-dots), have been widely explored as biomedical labeling reagents since 1998 [1–7]. The fluorescence of Q-dots is intrinsic, bright, and prolonged, and surpasses the sensitivity and resolution capability of organic dyes and proteins. During the past 10 years, type-II cadmium-based Q-dots have been widely used for fluorescence biological labeling [8,9]. However, experimental results indicate that any leakage of cadmium from the nanocrystals would be toxic and fatal to biological system [10–12]. For these reasons, numerous researches are currently conducted to develop Q-dots without any heavy-metal ions [13–15]. A new class of potential fluorescence material-doped semiconductor nanocrystals (D-dots), which are based on transition-metal-ion-doped D-dots without heavy-metal ions, can overcome the toxicity problems of traditional Q-dots mentioned above. Moreover, D-dots can potentially possess more unique properties, that is, zero reabsorption, high temperature stability, and reduced chemical sensitivity [14]. Among them, Mn-doped ZnS D-dots have been studied because it exhibited a typical

photoluminescence from the $\text{Mn}^{2+} \ ^4\text{T}_1 \rightarrow \ ^6\text{A}_1$ transition centered at about 595 nm [16,17]. Since biomedical fluorescence imaging, especially noninvasive in vivo imaging, requires deep penetration of light into and out of tissues, and the best penetration is achieved by light with a near-infrared wavelength ranging from 600 to 1000 nm [18,19], Mn-doped ZnS D-dots may become a new class of practical fluorescence biological labeling.

It is well known that the accessibility of Q-dots to serum albumins opens the door to understanding the binding mechanism of albumins with Q-dots and provides clues to the essential binding phenomenon [20,21]. In this work, chitosan (CS), a deacetylated derivative of chitin, the second most abundant biopolymer in nature [11,22], was used in the synthesis of Mn-doped ZnS (CS@ZnS:Mn) D-dots. Bovine serum albumin (BSA), one of the most extensively studied serum albumins, was selected as target serum albumin to study the interaction of CS@ZnS:Mn D-dots with proteins by using absorption and fluorescence methods. The quenching constants (K_{SV} and K'_{SV}), apparent binding constant (K_A), and number of binding sites (n) were obtained. Generally, most of the Q-dots present strong photochemical activity [20,21,23]. They respond well to ultraviolet (UV) illumination and produce reactive oxygen species (ROS), such as singlet molecular oxygen ($^1\text{O}_2$) and hydroxyl radical ($\cdot\text{OH}$), showing strong illuminated damage ability. Thus, the illumination damages of BSA molecule in the presence

* Corresponding author.

E-mail addresses: 2476625723@qq.com, liuli5058@aliyun.com (L. Liu).

of CS@ZnS:Mn D-dots were also studied. Some influencing factors such as illumination time and CS@ZnS:Mn D-dots concentrations were investigated systemically. It is hoped that this work could offer some valuable information to the applications of D-dots.

2. Experimental

2.1. Materials

CS with molecular weight of $6.0 \times 10^5 \text{ g mol}^{-1}$ and deacetylation degree of 87% was obtained from Zhejiang Yuhuan Jingke Biology Co., Ltd, China. Commercially prepared BSA was obtained from Wuhan Huashun Biological Technology Co., Ltd, China. $\text{Zn}(\text{OAc})_2 \cdot 2\text{H}_2\text{O}$, $\text{Mn}(\text{OAc})_2 \cdot 4\text{H}_2\text{O}$, HAC, and $\text{Na}_2\text{S} \cdot 9\text{H}_2\text{O}$ were obtained from Tianjin Bodi chemical Co., Ltd, China.

All chemicals were of analytical reagent grade and used without purification.

2.2. Apparatus and instruments

Ultraviolet–visible (UV–vis) absorption spectra were recorded on a UV-1601 spectrophotometer. The fluorescence emission (FL) spectra were measured using a Hitachi F-4500 fluorescence spectrophotometer with a Xe lamp as the light source. X-ray powder diffraction (XRD) analysis was recorded using a Bruker D8 Advance X-ray diffractometer with Cu K α irradiation. The elementary analysis was carried out at an Energy Dispersion Spectrum (EDS). The actual concentration of $[\text{Mn}^{2+}]$ encapsulated in CS@ZnS:Mn D-dots was measured using inductively coupled plasma atomic emission spectroscopy (ICP-AES).

2.3. Synthesis of CS@ZnS:Mn D-dots

CS@ZnS:Mn D-dots were synthesized by a precipitation method similar to that reported in the literature [24,25]. Briefly, 40 mL solution of $\text{Zn}(\text{OAc})_2$ (0.1 mol L^{-1}) and $\text{Mn}(\text{OAc})_2$ (0.05 mol L^{-1}) was mixed together in a beaker and stirred for 15 min. Then to this reaction mixture 40 mL CS solution (3.0 mg mL^{-1}) was added slowly. The solution was stirred for half an hour at 100°C . CS@ZnS:Mn D-dots were formed by adding 40 mL solution of Na_2S (0.1 mol L^{-1}) freshly prepared to the reaction mixture. The reaction was completed in 3.0 h, and CS@ZnS:Mn D-dots were precipitated at 10,000 rpm for 5 min, washed and resuspended in deionized water.

2.4. Measurement of binding parameters

BSA solution with the concentration of $1.5 \times 10^{-3} \text{ mmol L}^{-1}$ was prepared in Phosphate Buffered Saline buffer solution (PBS,

pH = 7.4). To a 10 mL colorimeter tube, 5 mL BSA stored solution and appropriate volume of CS@ZnS:Mn D-dots solution were added and diluted to the mark with PBS buffer solution, separately. The final BSA concentration was $7.5 \times 10^{-4} \text{ mmol L}^{-1}$ and the concentration of CS@ZnS:Mn D-dots was varied from 0.0 to 1.2 mmol L^{-1} at 0.1 mmol L^{-1} ($[\text{Mn}^{2+}]$) intervals. All test solutions were incubated for 30 min before measurement at different temperatures (293–313 K). The FL spectra of BSA in the absence and presence of CS@ZnS:Mn D-dots were recorded at excitation and emission wavelength of 286 and 350 nm, respectively. The FL spectra of CS@ZnS:Mn D-dots in the absence and presence of BSA were recorded at excitation and emission wavelength of 332 and 595 nm, respectively. The UV–vis absorption spectra of the corresponding solutions were also recorded in the range of 200–800 nm.

2.5. Determination of illumination damage procedure

Firstly, six clean 10 mL colorimeter tubes were marked as 1–6, respectively. Four 5 mL BSA solutions with a concentration of $1.5 \times 10^{-3} \text{ mmol L}^{-1}$ were taken exactly and put into colorimeter tubes 1, 2, 4, and 5, respectively. And then four 1 mL of CS@ZnS:Mn D-dots solution with concentration of 1.0 mmol L^{-1} were added to colorimeter tubes 2, 3, 5, and 6, respectively. Finally, all of the colorimeter tubes were diluted to 10 mL with PBS buffer solution, respectively. Then the tubes 4, 5, and 6 were placed directly under UV illumination, and the tubes 1, 2, and 3 were stored away from light. After illumination or placement, the UV–vis and FL spectra of all the samples were determined.

Illumination time was altered to 0–8 h and CS@ZnS:Mn D-dots concentrations were changed from 0.0 to 1.2 mmol L^{-1} at 0.1 mmol L^{-1} intervals, the influences on the illumination damages of BSA were investigated.

3. Results and discussion

3.1. Synthesis of CS@ZnS:Mn D-dots

Fig. 1a shows XRD patterns of CS@ZnS:Mn D-dots. CS@ZnS:Mn D-dots displayed some obvious peaks at 2θ values of 27.8° , 47.6° , and 57.5° , assigned to the ZnS cubic phase (111), (220), and (311) crystal planes. EDS spectrum of CS@ZnS:Mn D-dots, shown in Fig. 1b, revealed their elemental composition. It can be seen that, C, Zn, Mn, and S can be found from the spectral peaks. CS@ZnS:Mn D-dots were successfully obtained.

As is seen in Fig. 2, using an excitation wavelength of 332 nm, an emission peak centered at 595 nm was observed in CS@ZnS:Mn D-dots. Moreover, good linear relationship between the FL intensity of CS@ZnS:Mn D-dots and their concentration in the $0.1\text{--}2.0 \text{ mmol L}^{-1}$

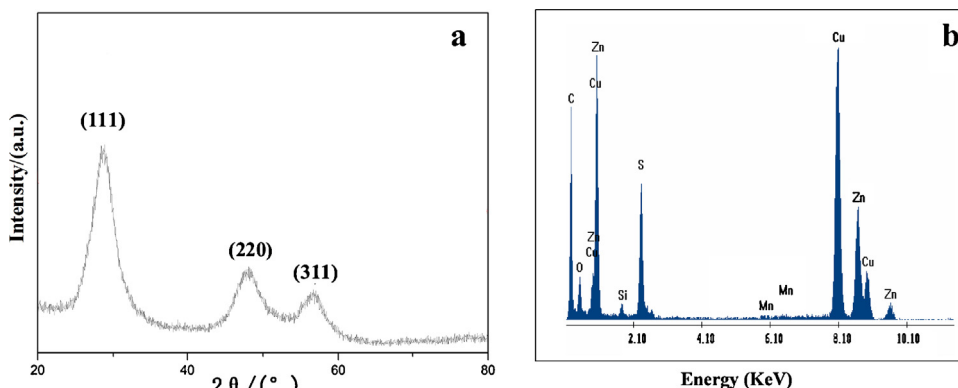


Fig. 1. XRD patterns (a) and EDS spectrum (b) of CS@ZnS:Mn D-dots.

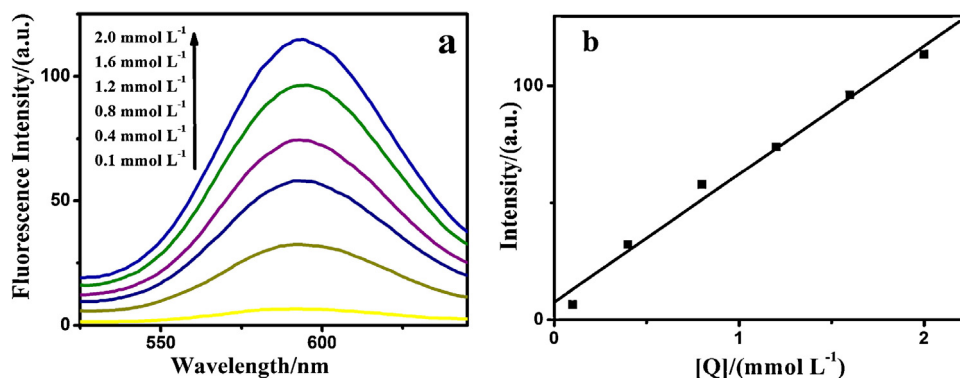


Fig. 2. FL spectra of CS@ZnS:Mn D-dots (a) and their FL property dependence on nanoparticles concentration (b).

concentration range was obtained (Fig. 2b). It revealed that CS@ZnS:Mn D-dots were uniformly dispersed in aqueous solution in a large concentration range. Along with a serial representative emission spectrum at different concentration of CS@ZnS:Mn D-dots in water, no emission spectra band shift was observed.

3.2. Spectroscopic studies of CS@ZnS:Mn-BSA interaction

In the present study, the UV-vis absorption and FL spectra of BSA in the absence and presence of CS@ZnS:Mn D-dots were recorded. As shown in Fig. 3a, the absorption of BSA at 286 nm increased with the increase in the addition of CS@ZnS:Mn D-dots in the 0.0–1.2 mmol L⁻¹ concentration range. Meanwhile, the intrinsic FL of BSA at 350 nm is gradually quenched along with the increase of CS@ZnS:Mn D-dots concentration (Fig. 3b). This result can be illustrated by the interaction of CS@ZnS:Mn D-dots with BSA.

The Stern-Volmer equation (Eq. (1)) [26] and modified Stern-Volmer equation (Eq. (2)) [27] were utilized to process the fluorescent data, obtained at three temperatures (293, 303, and 313 K), to clarify the FL quenching mechanism of BSA induced by CS@ZnS:Mn D-dots.

$$\frac{F_0}{F} = 1 + K_{SV}[Q] = 1 + \tau_0 K_q [Q] \quad (1)$$

$$\left(\frac{F_0}{F_0 - F} \right) = \frac{1}{f_a} + \left(\frac{1}{f_a K'_{SV} [Q]} \right) \quad (2)$$

where F_0 and F are the FL intensity of BSA in the absence and presence of CS@ZnS:Mn D-dots, respectively, $[Q]$ is the concentration of CS@ZnS:Mn D-dots, τ_0 is the lifetime of the fluorophore (usually 10^{-8} s), K_q is the bimolecular quenching rate constant, f_a is the fractional maximum FL intensity of BSA, and K_{SV} and K'_{SV} are the quenching constants at the corresponding temperature.

The K_q could be calculated according to equation $K_q = K_{SV}/\tau_0$ or K'_{SV}/τ_0 . If the value of K_q is apparently much larger than 2.0×10^{10} (mol L⁻¹)⁻¹s⁻¹, and the quenching constant values are inversely correlated with temperature, the quenching process could be concluded resulting from static compound formation. If not, the quenching mechanism is dynamic quenching.

The binding constant (K_A) and the binding sites number (n) at each temperature can be evaluated from the Double logarithm regression curve of $\log[(F_0 - F)/F]$ versus $\log [Q]$ based on the following equation [28]:

$$\log \left(\frac{F_0 - F}{F} \right) = \log K_A + n \log [Q] \quad (3)$$

where F_0 , F , and $[Q]$ have the same meanings of Eq. (1).

Fig. 4 displays the Stern-Volmer plots, modified Stern-Volmer plots, and Double logarithm plots of BSA with CS@ZnS:Mn D-dots at 293, 303, and 313 K, respectively. The resulting K_{SV} , K'_{SV} , K_q , K_A , and

Table 1

Quenching constant (K_{SV}), bimolecular quenching rate constant (K_q), binding constant (K_A), and number of binding sites (n) for interaction of BSA with CS@ZnS:Mn D-dots at different temperatures.

System	CS@ZnS:Mn-BSA		
Temperature (K)	293	303	313
K_{SV} ((mol L ⁻¹) ⁻¹)	1.824×10^3	1.87×10^3	2.061×10^3
K_q ((mol L ⁻¹) ⁻¹ s ⁻¹)	1.824×10^{11}	1.87×10^{11}	2.061×10^{11}
R^2	0.9951	0.996	0.9959
K_A	3.34×10^2	1.23×10^2	2.26×10^1
n	1.0864	0.9465	0.6825
R^2	0.9931	0.9936	0.9975

n values for the interaction between BSA and CS@ZnS:Mn D-dots at different temperatures are listed in Table 1.

In the present case, the Stern-Volmer plot of CS@ZnS:Mn-BSA sample exhibited a good linear relationship. The K_{SV} values of CS@ZnS:Mn-BSA are positively correlated with temperature. Hence, the dominating quenching mechanism of CS@ZnS:Mn-BSA binding might be initiated by dynamic quenching. The average number of binding sites for CS@ZnS:Mn D-dots per molecule of BSA is 0.906, equal to 1, indicating that there is one class of binding site for CS@ZnS:Mn D-dots to BSA molecule. To elucidate the nature of interaction between CS@ZnS:Mn D-dots with BSA, the thermodynamic parameters were calculated from the van't Hoff plots at three temperatures (293, 303, and 313 K) [29]. Both the enthalpy change (ΔH) and entropy changes (ΔS) can be evaluated, as:

$$\ln K_{SV} = -\frac{\Delta H}{RT} + \frac{\Delta S}{R} \quad (4)$$

The free energy change (ΔG) was then estimated from the following relationship:

$$\Delta G = \Delta H - T\Delta S = -RT \ln K_{SV} \quad (5)$$

where K_{SV} is the quenching constant at the corresponding temperature, R is the universal gas constant $8.314 \text{ J mol}^{-1} \text{ K}^{-1}$, and T is the temperature.

The resulting values of ΔH , ΔS , and ΔG are listed in Table 2. The negative values of ΔG reveal that the CS@ZnS:Mn-BSA binding processes are spontaneous. The positive values of ΔH and ΔS display that the hydrophobic interaction play major role in the CS@ZnS:Mn-BSA interaction.

Table 2

Thermodynamic parameters for interaction of BSA with CS@ZnS:Mn D-dots.

Temperature (K)	ΔG (kJ mol ⁻¹)	ΔH (kJ mol ⁻¹)	ΔS (J mol ⁻¹ K ⁻¹)
293	-18.13		
303	-19.03	8.009	89.03
313	-19.92		

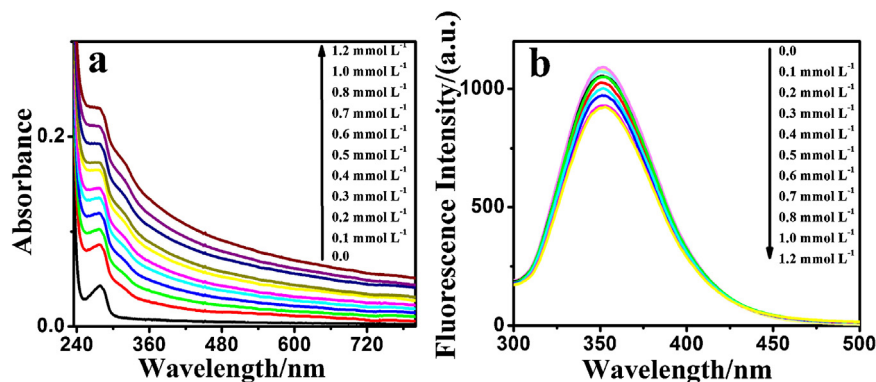


Fig. 3. UV-vis absorption (a) and FL spectra (b) of BSA in the absence and presence of CS@ZnS:Mn D-dots.

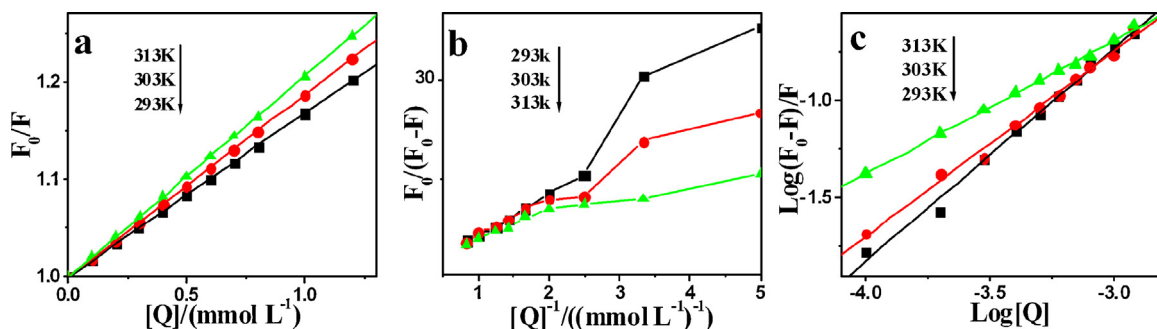


Fig. 4. Stern-Volmer plots (a), modified Stern-Volmer plots (b), and Double logarithm plots (c) of BSA with CS@ZnS:Mn D-dots concentration (from 0.0 to 1.2 mmol L⁻¹ at 0.1 mmol L⁻¹ intervals) at 293, 303, and 313 K.

3.3. The illumination damages of CS@ZnS:Mn D-dots to BSA molecule

Fig. 5a shows that the pure BSA solution has only one strong absorption peak at 286 nm. When BSA was mixed with CS@ZnS:Mn D-dots, the remarkable increase of the absorption peak at 286 nm was observed. After UV illumination, the solution shows much higher absorbance than the corresponding ones without UV illumination. Meanwhile, as shown in Fig. 5b, without UV illumination, the FL intensity of BSA at 350 nm in CS@ZnS:Mn-BSA system is quenched compared with that of the pure BSA. Under UV illumination, the FL intensity of BSA in CS@ZnS:Mn-BSA and the pure BSA all decreases, and show much lower FL intensity than the corresponding ones without UV illumination. The experiment results indicate that there is obvious

synergic effect of CS@ZnS:Mn D-dots and UV illumination on the damage of BSA.

The effects of illumination time on damages of BSA in the presence and absence of CS@ZnS:Mn D-dots were studied. Fig. 6a shows the absorbance changes (at 286 nm) of pure BSA and CS@ZnS:Mn-BSA with illumination time. It can be seen that the absorbance of BSA all increases along with the increase of illumination time in the presence and absence of CS@ZnS:Mn D-dots. From Fig. 6b it can be seen that, little decrease of FL intensity of pure BSA solution was found with or without UV illumination in 2.0 h in the presence and absence (at nitrogen atmosphere) of oxygen. In the presence of CS@ZnS:Mn D-dots and away from light, the FL intensity of CS@ZnS:Mn-BSA decreased gradually in the first 0.5 h, and then kept steady. Under UV illumination at nitrogen atmosphere, the FL intensity was gradually decreased to zero in more

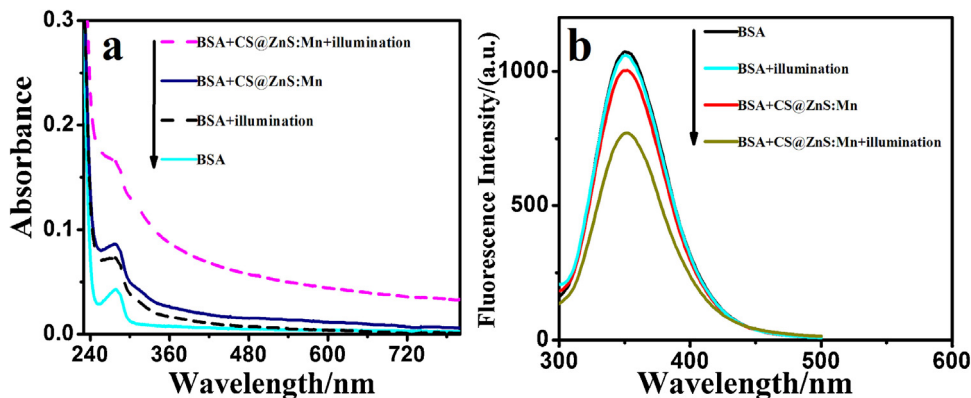


Fig. 5. UV-vis absorption (a) and FL spectra (b) of BSA and CS@ZnS:Mn-BSA under different condition ([BSA] = 7.5×10^{-4} mmol L⁻¹, [CS@ZnS:Mn] = 0.1 mmol L⁻¹).

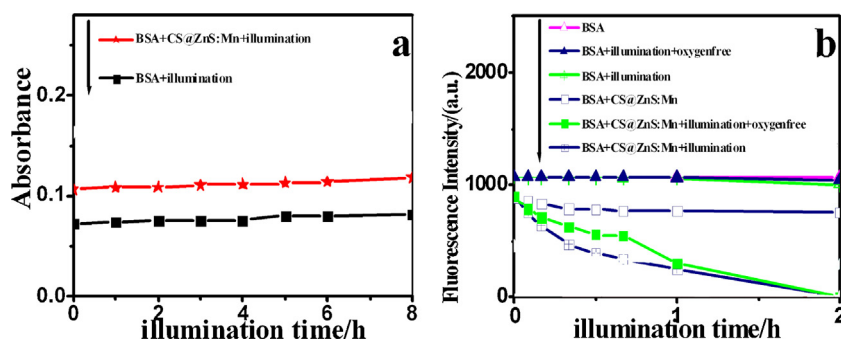


Fig. 6. Changes of UV-vis absorbance (a) and FL intensity (b) of BSA and CS@ZnS:Mn-BSA with illumination time (from 0.0 to 8.0 h).

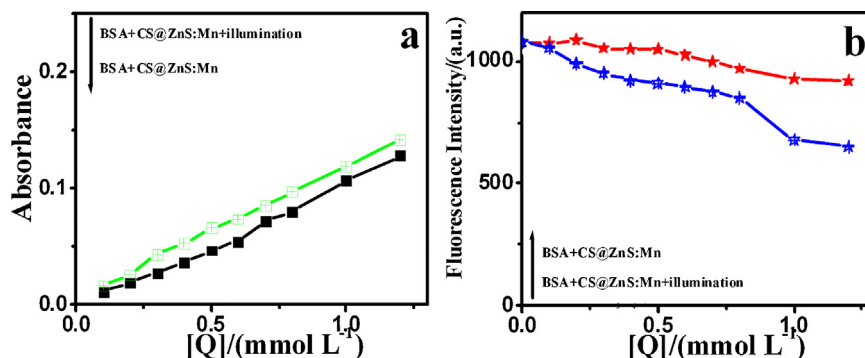


Fig. 7. Changes of UV-vis absorbance (a) and FL intensity (b) of BSA under different condition (with CS@ZnS:Mn D-dots concentration changed from 0.0 to 1.2 mmol L⁻¹).

than 2.0 h. Under UV illumination with air, the FL intensity was fleetly decreased to zero in less than 2.0 h. It means that the damage of the BSA molecule becomes more and more serious with the increase of illumination time.

It can be seen in Fig. 7a, the absorption peak of BSA solution all increases with the increase of CS@ZnS:Mn D-dots concentration. For the same concentration, the absorption is obviously higher under UV illumination than that without UV illumination. That is, on the basis of interaction, the BSA molecule is further damaged in the presence of CS@ZnS:Mn D-dots under UV illumination. The influences of CS@ZnS:Mn D-dots concentration are also studied by FL spectra. Fig. 7b shows that, the FL intensity of BSA solution decreases along with the increase of CS@ZnS:Mn D-dots concentration. For corresponding CS@ZnS:Mn D-dots concentration, the FL intensity of BSA solution under UV illumination is quenched more serious. It indicates that, CS@ZnS:Mn D-dots have a very significant positive influence on the damage of BSA under UV illumination.

The changes of FL intensity of CS@ZnS:Mn D-dots in the presence of BSA were also studied. Fig. 8 describes the effect of BSA on the FL intensity of CS@ZnS:Mn D-dots. The FL intensity all increases along with the increase of CS@ZnS:Mn D-dots concentration. There are good linear relationships between relative FL intensity and concentration of CS@ZnS:Mn D-dots in the absence and presence of BSA solution with and without UV illumination. Simultaneously, we found that the FL intensity of CS@ZnS:Mn D-dots is higher in the presence of BSA. After UV illumination in the presence of BSA, the FL intensity of CS@ZnS:Mn D-dots increased more.

The effects of illumination time on the FL spectra of CS@ZnS:Mn D-dots in the presence and absence of BSA solution were also studied (Fig. 9). It can be seen that, the FL intensity of pure CS@ZnS:Mn D-dots is constant in 1.0 h without UV illumination, and then decreases along with the increase of illumination time. However, the FL intensity of CS@ZnS:Mn D-dots all increases along with the increase of illumination time in the presence of BSA.

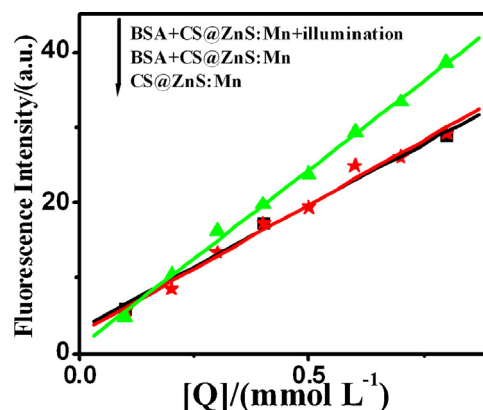


Fig. 8. Linear dependence of FL intensity with reciprocal concentration of CS@ZnS:Mn D-dots in the absence and presence of BSA ([BSA] = 7.5×10^{-4} mmol L⁻¹) with and without UV illumination.

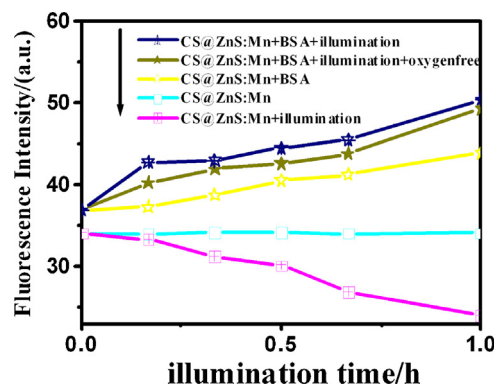


Fig. 9. Changes of FL intensity of CS@ZnS:Mn D-dots in the absence and presence of BSA ([BSA] = 7.5×10^{-4} mmol L⁻¹) with UV illumination time (from 0.0 to 1.0 h).

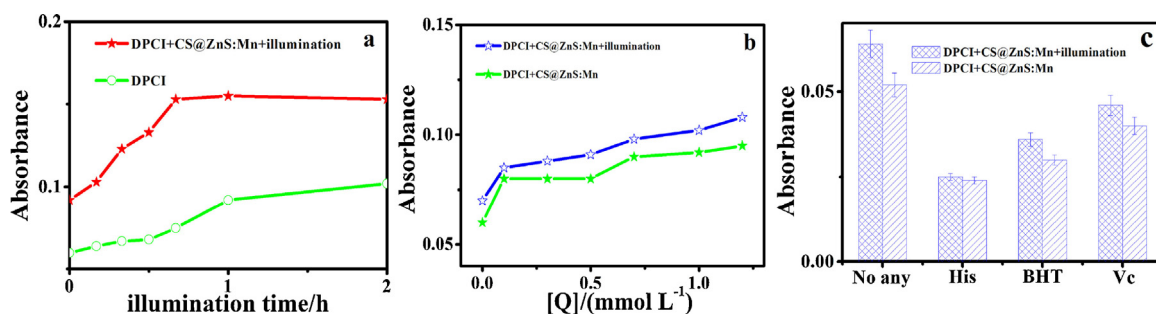


Fig. 10. Chances of UV–vis absorbance of DPCO generated from DPCI with illumination time (a) and CS@ZnS:Mn D-dots concentration (b), and various ROS quenchers (c). Data estimated from the average of $n = 3$ experiments, and error bars represent one standard deviation from the mean.

3.4. Mechanism discussion

CS@ZnS:Mn D-dots as photosensitizers was irradiated by UV illumination and the generated ROS was investigated by the method of Oxidation–Extraction Spectrometry (OEP) [20,30]. Fig. 10 shows that, the absorbance of diphenylcarbonzone (DPCO) generated from diphenylcarbonyl (DPCI) obviously increases along with the increase of illumination time and CS@ZnS:Mn D-dots concentration. Moreover, the hyperchromic effect is more obvious in the present of CS@ZnS:Mn D-dots. Generally, the L-Histidine (His) can quench the singlet state molecular oxygen (1O_2), the 2,6-Di-tert-butyl-methylphenol (BHT) can quench the hydroxyl radicals ($\cdot OH$), and the Vitamin C (Vc) can quench almost all kinds of ROS. Here, His, BHT, Vc are used to determine the kind of generated ROS. Fig. 10c shows that the absorbance of DPCO generated from DPCI is obviously weakened in different degrees after the addition of His, BHT, and Vc. This phenomenon estimates that CS@ZnS:Mn D-dots under UV illumination can lead to the generation of several kinds of ROS, at least including 1O_2 and $\cdot OH$, and the quantities of ROS increase with the increase of illumination time and CS@ZnS:Mn D-dots concentration.

It is well known that the $\cdot OH$ radical is a powerful oxidizing agent capable of degrading most biomolecules. According to investigations mentioned above, in the presence of CS@ZnS:Mn D-dots and UV illumination, a photo-induced free radical process for BSA damage would be expected. CS@ZnS:Mn D-dots form complex with BSA. The BSA free radicals could be produced in the system, the increases of FL intensity of CS@ZnS:Mn D-dots can be explained by further cross-linking and polymerization of the BSA molecule adsorbed on the surface of CS@ZnS:Mn D-dots, which results in a better passivation of surface states act as nonradiative recombination center [31].

4. Conclusion

In summary, the interaction studies of BSA with CS@ZnS:Mn D-dots as well as the illumination damages of CS@ZnS:Mn D-dots to BSA molecule were investigated by UV–vis absorption and FL spectra. According to the calculation of fluorescence quenching, the dominating quenching mechanism of CS@ZnS:Mn D-dots with BSA belongs to dynamic quenching. The hydrophobic interaction plays major roles in the CS@ZnS:Mn–BSA interaction, the binding processes are spontaneous. The coaction of CS@ZnS:Mn D-dots and UV illumination leads to more serious damages to BSA molecule.

The probable quenching mechanism is mainly a photo-induced free radical procedure. A proportionate quenching in BSA fluorescence is followed by an enhancement of CS@ZnS:Mn D-dots fluorescence. CS@ZnS:Mn D-dots may be potential candidate for application in biological studies. Our work provides some useful suggestions for D-dots' further investigations.

References

- [1] M. Bruchez, M. Moronne, P. Gin, S. Weiss, A.P. Alivisatos, *Science* 281 (1998) 2013–2016.
- [2] W.C.W. Chan, S. Nile, *Science* 281 (1998) 2016–2018.
- [3] W. Dong, L. Guo, M. Wang, S.K. Xu, *J. Lumin.* 129 (2009) 926–930.
- [4] A.M. Smith, H.W. Duan, A.M. Mohs, S.M. Nie, *Adv. Drug Deliv. Rev.* 60 (2008) 1226–1240.
- [5] J.C. Claussen, W.R. Algar, N. Hildebrandt, K. Susumu, M.G. Ancona, I.L. Medintz, *Nanoscale* 5 (2013) 12156–12170.
- [6] J.C. Claussen, N. Hildebrandt, K. Susumu, M.G. Ancona, I.L. Medintz, *ACS Appl. Mater. Int.* 6 (2014) 3771–3778.
- [7] J.C. Claussen, A. Malanoski, J.C. Breger, E. Oh, S.A. Walper, K. Susumu, R. Goswami, J.R. Deschamps, I.L. Medintz, *J. Phys. Chem. C* 119 (2015) 2208–2221.
- [8] G.F. Jie, L. Wang, J.X. Yuan, S.S. Zhang, *Anal. Chem.* 83 (2011) 3873–3880.
- [9] L.N. Chen, J. Wang, W.T. Li, H.Y. Han, *Chem. Commun.* 48 (2012) 4971–4973.
- [10] A.M. Derfus, W.C.W. Chan, S.N. Bhatia, *Nano Lett.* 4 (2004) 11–18.
- [11] H.Y. Xia, G. He, J.X. Peng, W.W. Li, Y. Fang, *Appl. Surf. Sci.* 256 (2010) 7270–7275.
- [12] N. Chen, Y. He, Y.Y. Su, X.M. Li, Q. Huang, H.F. Wang, X.Z. Zhang, R.Z. Tai, C.H. Fan, *Biomaterials* 33 (2012) 1238–1244.
- [13] X.G. Peng, *Nano Res.* 2 (2009) 425–447.
- [14] N. Paradha, X.G. Peng, *J. Am. Chem. Soc.* 129 (2007) 3339–3347.
- [15] R. Zhang, Y.B. Liu, S.Q. Sun, *Appl. Surf. Sci.* 282 (2013) 960–964.
- [16] X.J. Wang, Q.L. Zhang, B.S. Zou, A.H. Lei, P.Y. Ren, *Appl. Surf. Sci.* 257 (2011) 10898–10902.
- [17] R. Viswanath, H.H. Bhojya Naik, G.S. Yashavanth Kumar, P.N. Prashanth Kumar, K.N. Harish, M.C. Prabhakara, R. Praveen, *Appl. Surf. Sci.* 301 (2014) 126–133.
- [18] S.A. Hilderbrand, R. Weissleder, *Curr. Opin. Chem. Biol.* 14 (2010) 71.
- [19] L. Liu, L. Xiao, H.Y. Zhu, *Chem. Phys. Lett.* 539–540 (2012) 112–117.
- [20] L. Liu, L. Xiao, H.Y. Zhu, X.W. Shi, *J. Nanopart. Res.* 15 (2013) 1394.
- [21] L. Liu, L. Xiao, C.H. Cao, *Mater. Chem. Phys.* 140 (2013) 575–582.
- [22] C.H. Cao, L. Xiao, L. Liu, H.Y. Zhu, C.H. Chen, L. Gao, *Appl. Surf. Sci.* 271 (2013) 105–112.
- [23] L.C. Ann, S. Mahmud, S.K.M. Bakhori, A. Sirelkhatim, D. Mohamad, H. Hasan, A. Seeni, R.A. Rahman, *Appl. Surf. Sci.* 292 (2014) 405–412.
- [24] K. Manzoor, S.R. Vadera, N. Kumar, T.R.N. Kutty, *Solid State Commun.* 129 (2004) 469–473.
- [25] M. Sharma, S. Singh, O.P. Pandey, *J. Appl. Phys.* 107 (2010) 104319.
- [26] O.R. Quayle, *Chem. Rev.* 53 (1953) 439–589.
- [27] S.S. Lehrer, *Biochemistry* 10 (1971) 3254–3263.
- [28] H. Gao, L. Lei, J.Q. Liu, Q. Kong, X.G. Chen, Z.D. Hu, *J. Photochem. Photobiol. A: Chem.* 167 (2004) 213–221.
- [29] O. Khani, H.R. Rajabi, M.H. Yousefi, A.A. Khosravi, M. Janesari, M. Shamsipur, *Spectrochim. Acta A* 79 (2011) 361–369.
- [30] J. Wang, Y.W. Guo, B. Liu, X.D. Jin, L.J. Liu, R. Xu, Y.M. Kong, B.X. Wang, *Ultrason. Sonochem.* 18 (2011) 177–183.
- [31] C. Carrillo-Carrion, S. Cardenas, B.M. Simonet, M. Valcarcel, *Chem. Commun.* (2009) 5214–5226.